Study of the Effects of Melt Blending Speed on the Structure and Properties of Phosphate Glass/Polyamide 12 Hybrid Materials

Kevin Urman, Douglas Iverson, Joshua U. Otaigbe

School of Polymers and High Performance Materials, University of Southern Mississippi, Hattiesburg, Mississippi 39406-0076

Received 16 March 2006; accepted 20 July 2006
DOI 10.1002/app.25266
Published online 23 April 2007 in Wiley InterScience (www.interscience.wiley.com).

ABSTRACT: The effects of melt blending conditions on the rheology, crystallization kinetics, and tensile properties of phosphate glass/polyamide 12 hybrid systems were investigated for the first time, to understand their complex processing/structure/property relationships. Increasing amounts of phosphate glass (Pglass) caused an increase in hybrid viscosity. Hybrid viscosity was also affected by processing (melt-mixing) speed and small-amplitude oscillatory shear tests and scanning electron microscopy (SEM) were used for a qualitative examination of the hybrid morphology. The addition of Pglass caused a decrease in hybrid crystallinity that was unaffected by processing (melt-mixing) speed. The two-parameter Avrami equation was applied successfully to the hybrid systems, and Pglass was found to nucleate the growth of polyamide 12 crystals. The nucleation effect was found to be dependent on concentration and processing history. The tensile properties of the hybrids were also studied, and the Halpin–Tsai equation was applied to the results to determine the maximum packing fraction of the Pglass. These results provide a basis for the prediction of hybrid mechanical properties for different Pglass concentrations and processing histories. Further, because of their facile processibility and desirable characteristics, such as the strong physicochemical interaction between the hybrid components and favorable viscoelasticity, these Pglass/polyamide 12 hybrids can be used as model systems for exploring feasibility of new routes for driving organic polymers and inorganic Pglass to self-assemble into useful organic/inorganic hybrid materials. J Appl Polym Sci 105: 1297–1308, 2007

Key words: heterogeneous polymers; phosphate glass/polyamide 12 hybrids; morphology and property; processing and rheology; crystallization

INTRODUCTION

Polymer/polymer blending and polymer reinforcement with inorganic fillers are two common methods of creating new materials with tailored properties for emerging applications. In the polymer industry, utilization of the former approach (i.e., polymer/polymer blending) has seen considerable growth over the past 20 years because of its relatively low cost as compared with synthesizing a new polymer.[1] As an additional benefit, blending of two or more polymers can have synergistic effects that can create a substantially better material than the pure polymer components. However, the currently available commercial polymer blend materials cannot satisfy the growing need for new advanced materials. This need is being addressed in part by inorganic/organic hybrid materials. Hybrid materials are defined as synthetic materials that contain both organic and inorganic components.[2,3] They can be further classified into systems derived from monomers or miscible components, homogeneous systems, and phase-separated or heterogeneous systems.[2,3] A relatively unexplored class of heterogeneous hybrids are the phosphate glass/polymer hybrids. These materials are mixtures of an ultra-low glass transition (T_g) phosphate glass (Pglass) and an organic polymer. Phosphate glasses that display both water resistance and chemical durability are now readily available.[4,5] One such Pglass is tin fluorophosphate glass with a T_g of $\sim 125^{\circ}C$, which is known to be extremely resistant to water and chemical degradation.[6–8] With such a low T_g, it is possible to blend these Pglasses with organic polymeric materials, using conventional processing methodologies to yield hybrid materials containing Pglass loadings of 60% by volume or 90% by weight, thereby eliminating the intractable viscosity problem inherent to conventional polymer composites at high solid filler compositions. Because both the organic polymer and Pglass components are fluid during processing, it is possible to obtain a variety of morphologies and significant improvements in

Correspondence to: J. U. Otaigbe (joshua.otaigbe@usm.edu).
Contract grant sponsor: Division of Materials Program/US National Science Foundation; contract grant numbers: DMR 97-33350, 03-09115.

Journal of Applied Polymer Science, Vol. 105, 1297–1308 (2007)

properties that are impossible to achieve from classical polymer blends and composites.

Although Pglass/polymer hybrids are significantly different from conventional polymer composites and blends, a number of the theories developed for classical polymer composites and blends are conjectured to be applicable to the present hybrid system. For instance, it is widely accepted that the final properties of a blend or mixture depend on the pure components' properties, composition, interfacial tension, and morphology.[1,9,10] In turn, the morphology of the blend is influenced by the processing history of the material. Microstructural evolution during processing of a blend is a complex phenomenon that is not yet fully understood. Lee and Han[11] showed that by increasing the processing temperature or the speed of mixing, it was possible to achieve a stable morphology in a short time. Other reported studies have found that by increasing the mixing speed, a reduction in the size of the dispersed phase is observed.[12,13]

During the physical compounding of a polymer blend, another important process that affects the final blend morphology is the breakup and coalescence of the dispersed phase. Droplet coalescence, which may be responsible in part for the results reported by Lee and Han, mentioned above, is essentially a four-step process that initially involves a pair of particles brought into close proximity with each other. The pair of particles rotates together in the flow field and is separated by a thin film. During the particle rotation, the thin film drains away due to viscous flow. If the film thickness is reduced sufficiently, the particles can coalesce.[14] The amount and rate of coalescence that occurs is dependent on several factors, including concentration, viscosity ratios, shear rate, and size of the discrete phase.[15,16]

Although the complex interplay between the processing conditions, material parameters, and droplet breakup and coalescence is not fully understood, by systematically varying the blend concentration and processing conditions such as melt-mixing speed (or shear rate), one can begin to elucidate the complex processing/structure/property relationships within a blend. Applying this methodology to the Pglass/polymer hybrids can provide the knowledge needed to tailor the hybrid morphology and properties in unprecedented ways through carefully controlled processing and, in turn, provide a basis for further theory development and a better understanding of the behavior of these materials. As these hybrids are an emerging class of materials, only a handful of systems have been investigated.[17–21] The present study extends the reported prior work into Pglass/polyamide 12 hybrids, where the physical and chemical interactions between —OH (from Pglass) and the $—NH_2$ (from polyamide 12) chemical functional groups of the hybrid components are significantly increased. The present work emphasizes the dependence of the rheological, crystalline, and tensile properties on processing history and the resultant morphology over a wide range of compositions. To our knowledge, this is the first attempt to study systematically the effect of varying processing conditions on properties for these special hybrid materials. As part of our long-range research program in this field, modern solid-state nuclear magnetic resonance (NMR) methods are being used to provide useful information on composition, nanometer-scale mixing, and dynamics in the hybrid systems; the results obtained will be reported elsewhere.[22] The favorable chemical interactions between the hybrid components and their mixing in the liquid state will enhance the mechanical properties of the Pglass/polyamide 12 hybrids for a number of applications, making the present hybrid system useful model systems for exploring feasibility of new processing routes for driving organic polymers and inorganic phosphate glasses to self-assemble into useful hybrid materials.

EXPERIMENTAL

The low T_g Pglass used in this study has a molar composition of 50% SnF_2 + 20% SnO + 30% P_2O_5, a density of 3.75 g/mL, and a T_g of 125.7°C. The Pglass was synthesized in our laboratory using procedures previously reported elsewhere.[23] The tin fluoride and tin oxide were supplied by Cerac (Milwaukee, WI) and the ammonium phosphate was supplied by Sigma-Aldrich (St. Louis, MO). The polyamide 12 (Vestamid® L1700) was supplied by Degussa AG (Düsseldorf, Germany). The density and melt flow index of the polyamide 12 are 1.02 g/mL and 120 g/10 min, respectively.

A ThermoHaake Polydrive® melt mixer with rotor roller blades was employed to melt-mix the hybrid components thoroughly before fabrication (i.e., compression and injection molding) of parts and test samples. The polyamide 12 and the Pglass were dried in a vacuum oven before melt-mixing. The Polydrive® mixer was preheated to 220°C for at least 20 min before mixing in order to ensure that the instrument had reached thermal equilibrium. Before any of the hybrid components were added to the mixer, the instrument was calibrated at the appropriate mixing speed. The polyamide 12 was first added to the Polydrive® mixing bowl and allowed to mix for 5 min to yield a homogeneous melt. The Pglass was subsequently added in the required amounts to the mixer and allowed to mix for an additional 10 min. Hybrids containing 10%, 20%, 30%, 40%, and 50% by volume of Pglass were prepared at rotor speeds of 50, 75, and 100 rpm. The hybrid materials were collected in ''chunks'' from the Polydrive® mixer for further processing.

Before further processing, the materials were dried in a vacuum oven. A portion of the melt-mixed

material was compression-molded into thin films for differential scanning calorimetry (DSC) studies described below. To conserve material, only hybrids containing 10%, 30%, and 50% Pglass were pressed into discs with a 25-mm diameter and 1.5-mm thickness for rheological measurements.

A Tetrahedron® Melt Press was used to prepare the compression-molded samples. The press was preheated to 220°C, and the hybrid material was allowed to melt in the press before a load of 1,000 psi (6.895 MPa) was applied. The material was kept at 220°C for 5 min before cooling to room temperature at 25°C/min. The molding pressure was then removed, and the samples were collected. Another portion of the melt-mixed material from the Polydrive® mixer was ground into fine particles for subsequent injection molding, using an IKA® A11 basic laboratory mill. The fine particles were injection-molded into either dog bone shapes (4.32 mm wide and 1.55 mm thick with a gauge length of 28.70 mm) or small rectangular bars, using a DACA Microinjector® equipped with the appropriate mold. A mold residence time of 10 s, a barrel temperature of 220°C, and a mold temperature of 40°C were used to obtain test samples with reproducible properties and no visible flaws.

All tested samples were dried for at least 48 h or until constant weight was achieved in a vacuum oven before testing. The morphology of the hybrids was examined using a FEI Quanta® 200 scanning electron microscope (SEM). Cross sections of the injection-molded bars and compression-molded discs were mounted onto aluminum posts, cryotomed, and gold sputtered before being examined by SEM. Rheological characterization was performed using a strain controlled ARES® rheometer. Testing was performed at 195°C to ensure a viscosity that was within the limits of the instrument. Higher temperatures gave viscosities too low to be measured reliably by the rheometer. A strain sweep was performed on each composition that was examined to determine the linear viscoelastic region. The linear viscoelastic region varied with composition and, therefore, linear strain amplitudes of 1%, 0.5%, and 0.1% were used for the 10%, 30%, and 50% Pglass hybrid systems, respectively, in the frequency sweep experiments. Several small-amplitude oscillatory shear measurements were then performed on each sample to ensure reproducibility; the mean results are similar to those reported in this article. Liquid nitrogen-cooled Perkin-Elmer Pyris Diamond® DSC was used to measure the crystalline properties of the hybrids. An Alliance RT/10® Material Testing System was used to investigate the tensile properties of the hybrids. The dog bone samples were conditioned in ambient conditions for 1 week prior to testing and the samples were deformed at a rate of 5.08 mm/min. Five samples were tested at each composition, and the values were averaged to obtain the final results reported in this article.

RESULTS AND DISCUSSION

Morphology

It has been previously shown that as-prepared (''chunk'') material from the Polydrive® mixer displays a decrease in Pglass particle size with increasing mixer rotor speed (or shear rate), which is consistent with theory.[24,25] However, the effect of rotor speed on morphology becomes more complicated upon injection or compression molding of the melt-mixed (''chunk'') material due to shear-induced coalescence and breakup. This effect is clearly seen in micrographs of the injection-molded samples (Fig. 1). Note that the Pglass content increases in volume percentage (vol %) from top to bottom of Figure 1 with the 10% Pglass/polyamide 12 hybrid as the first row [Fig. 1(a)–(c)] and the 50% Pglass/polyamide 12 hybrid as the last row [Fig. 1(g)–(i)]. Additionally, the Polydrive® melt-mixing speed increases from left to right as depicted in Figure 1. The 10 vol % hybrid displays small droplets of Pglass dispersed in the polyamide 12 matrix. This morphology is maintained regardless of the mixing speed used. If one considers only the hybrids prepared at 50 rpm, it is clearly evident that the droplet morphology is maintained over the whole range of hybrid compositions studied. However, it is easily seen in Figure 1 that as the volume of Pglass is increased, larger Pglass droplets are formed and there is visual evidence of coalescence in the micrographs. When the processing speed is increased to either 75 or 100 rpm, the effect of coalescence becomes more pronounced. For hybrids prepared at these higher speeds, large agglomerations of Pglass are seen starting at 20 vol % Pglass (not shown). As the Pglass content is increased further, the Pglass agglomerations continue to get larger, eventually forming a co-continuous or interpenetrating network-like morphology. This behavior is consistent with reported theoretical scaling models for droplet coalescence, which predict that small droplets are more likely to coalesce than large droplets and that increasing the volume fraction of the droplets increases the coalescence rate.[13]

It is noteworthy that when the hybrid materials are compression-molded, the morphology differs from that of injection-molded samples depicted in Figure 1. The observed morphologies of the compression-molded samples are shown in Figure 2; the 10% Pglass/polymer hybrid is in the first row [Fig. 2(a)–(c)], the 30% Pglass/polymer hybrid is in the second row [Fig. 2(d)–(f)], and the 50% Pglass/polymer hybrid is in the last row [Fig. 2(g)–(i)], while the speed

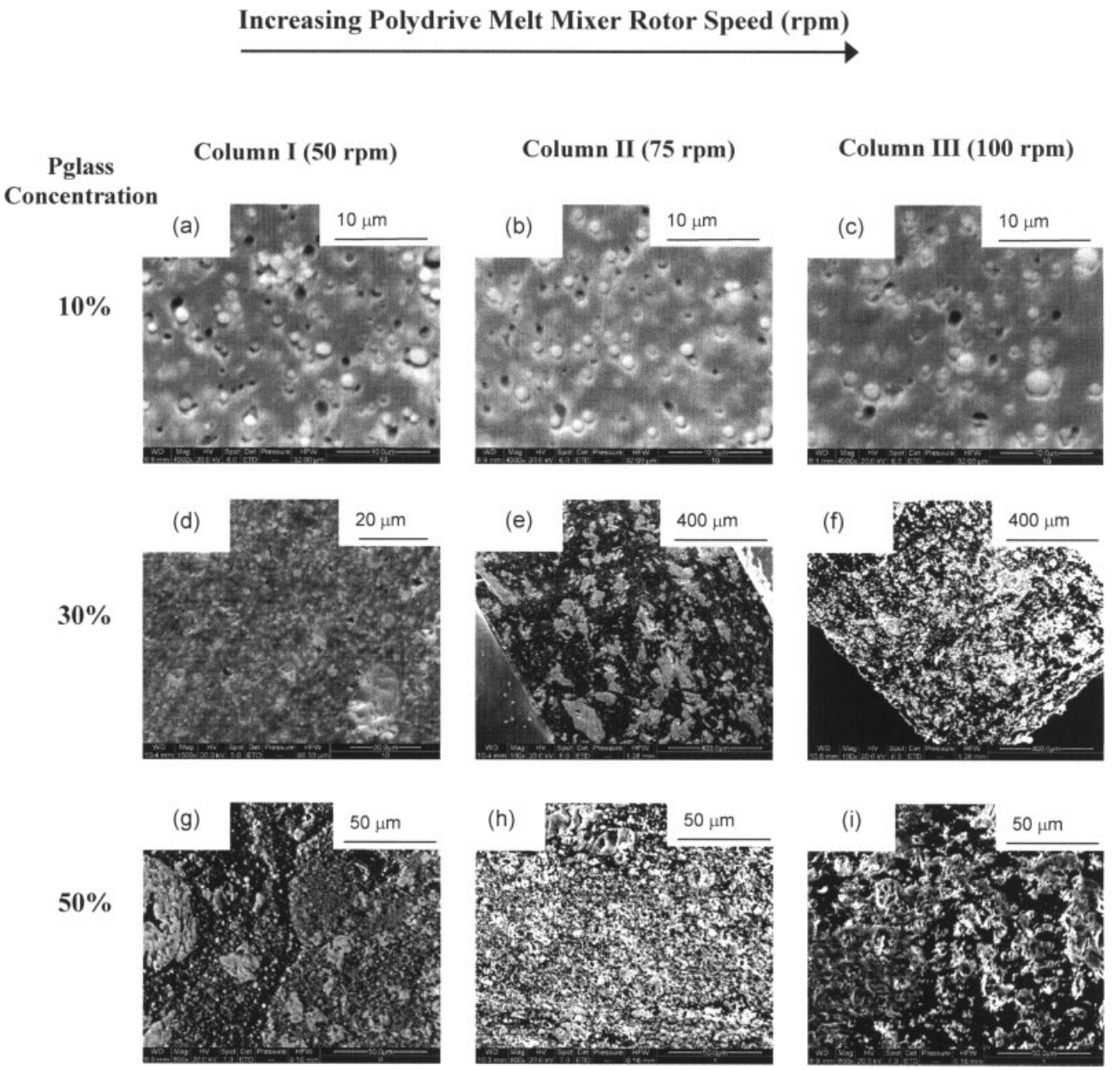

Figure 1 SEMs of injection-molded Pglass/polyamide 12 hybrids that were premixed at different melt-mixing speeds indicated.

at which the hybrids were melt-mixed in the Polydrive® mixer increases going from column I to column III, as indicated. The differences in morphology between compression-molded (Fig. 1) and injection-molded (Fig. 2) samples become more prominent as the concentration of Pglass increases in the hybrids. The 10 vol % Pglass/polymer hybrid samples show a droplet type morphology that is similar to that of the injection-molded samples, with some slight evidence of coalescence. As the vol % of Pglass is increased to 30%, the droplet morphology is maintained, but there is an increasing amount of Pglass droplet coalescence. When this sample is compared with the injection-molded sample already discussed, it is easy to see that more Pglass droplet coalescence occurs during injection molding for this 30% Pglass/polymer hybrid composition. The 50% Pglass/polymer hybrids display a very different morphology to an extent that depends on the rotor speed (or shear rate) used to melt-mix the hybrid in the Polydrive® mixer. For example, the hybrid sample melt-mixed at 50 rpm shows a significant degree of Pglass droplet coalescence, but there are still a large number of small droplets in the system, as Figure 2 shows. The 50% Pglass/polymer hybrids melt-mixed at 75 rpm and 100 rpm display large agglomerated structures that are typical of co-continuous type morphologies. The morphology corresponding to the sample melt-mixed at 75 rpm is

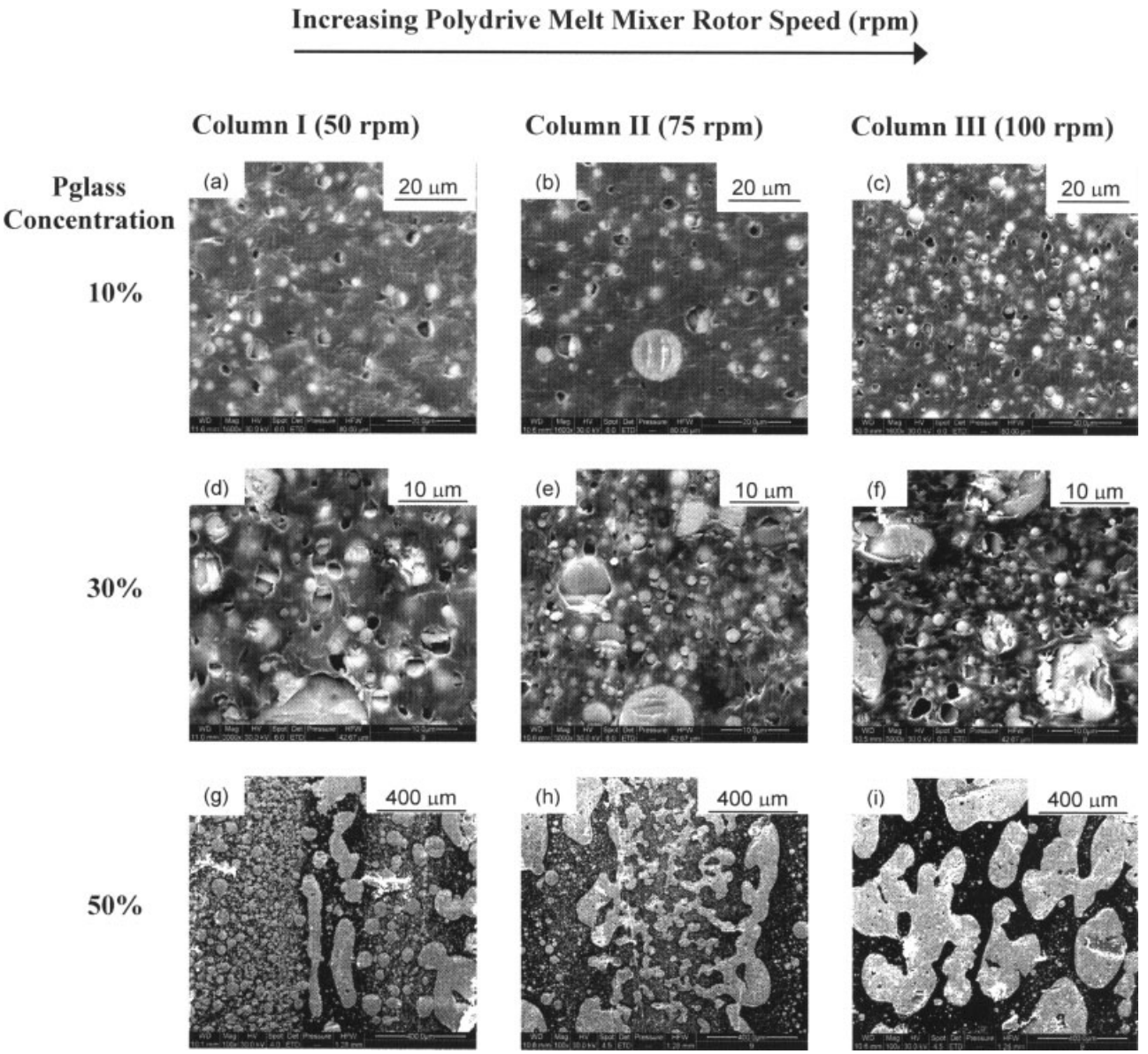

Figure 2 SEMs of compression-molded Pglass/polyamide 12 hybrids that were premixed at different melt-mixing speeds indicated.

finer and more connected than that of the sample melt-mixed at 100 rpm.

The observed differences in morphology between compression-molded and injection-molded samples can be rationalized based on the different amount of shear and mold residence (heating) time experienced by the material during the different molding processes with varying melt deformation environment and histories. During compression molding, the material is subjected to relatively lower shear and more mold residence time at elevated temperature with respect to injection molding. While the lower shear rate the material experiences during compression molding will decrease the capillary number and should in theory favor coalescence, the longer mold residence time at elevated temperature provides more time for the material to relax and change the shear-induced morphology.

Viscoelasticity

By examining these materials using small-amplitude oscillatory shear flow experiments, the morphology of the hybrids and its influence on viscoelastic properties can be further probed. Figure 3 shows the complex viscosity of compression-molded hybrids as a function of frequency for all the Polydrive® melt-mixing speeds used in this study. Regardless of Polydrive® melt-mixing speed used, the complex viscosity is shown to increase with increasing Pglass content, consistent with Taylor's theory.[26] More information concerning the effect of the Polydrive®

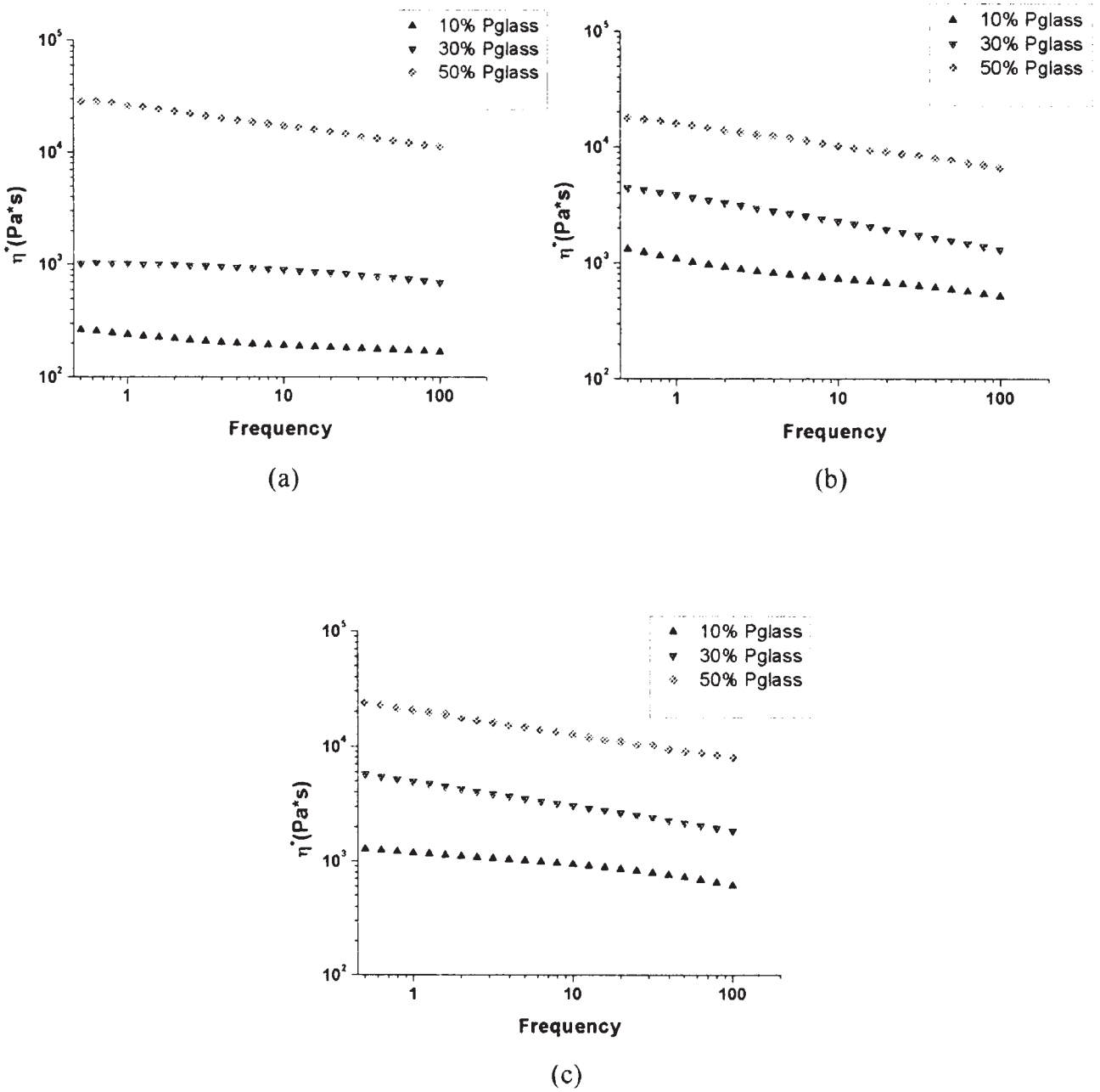

Figure 3 Complex viscosity of typical hybrids as a function of frequency for hybrids that were premixed at melt-mixing speeds of 50 rpm (a), 75 rpm (b), and 100 rpm (c).

melt-mixing speed on the rheology of these materials can be seen in Figure 4, which compares the frequency dependence of storage modulus for the individual hybrid compositions that were melt-mixed at the different speeds indicated. It has been shown that storage modulus increases with decreasing dispersed phase size.[9] In Figure 4(a), the hybrids containing 10 vol % Pglass that were prepared at 75 rpm and 100 rpm show similar storage moduli, implying that these two hybrids have similar microstructures. A similar trend is shown in Figure 4(b) for the 30 vol % Pglass compositions prepared at 75 rpm and 100 rpm. In addition, the dispersed phase in these hybrids is observed to be smaller than that of the hybrids prepared at 50 rpm. The small Pglass droplet sizes, which dominate the rheology of these systems, were measured and found to be consistent with the analysis of the frequency dependence of the storage modulus as shown in Table I.

The observed trend in the viscoelastic material functions of the hybrids with low Pglass concentration hybrids (10% and 30% Pglass) discussed above changes when the 50% Pglass/polymer hybrid was examined. The 50% Pglass/polymer hybrid prepared using a Polydrive® mixer at 50 rpm displays the highest storage modulus, while the hybrid prepared

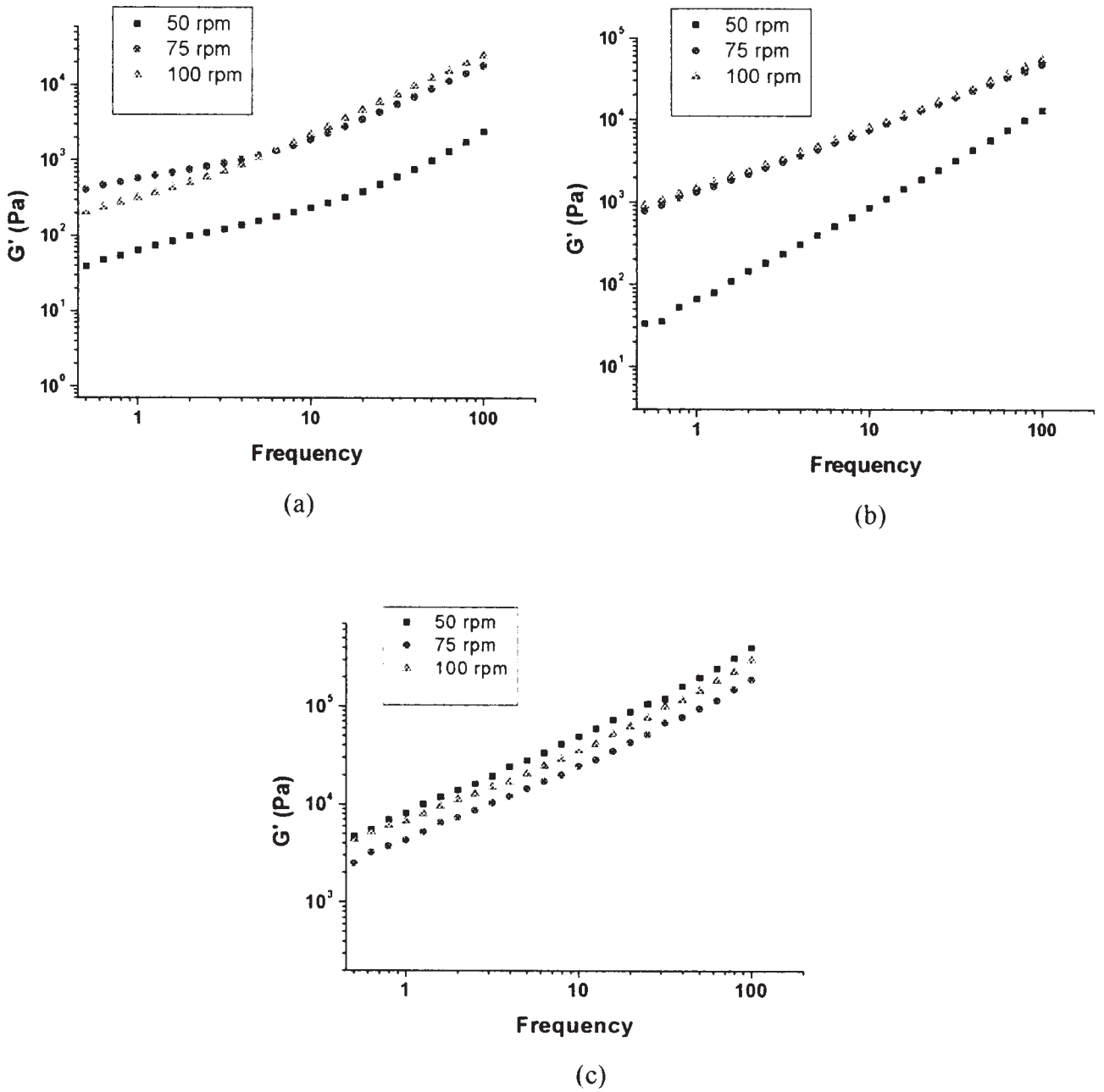

Figure 4 Frequency dependence of storage modulus for: (a) 10 vol % Pglass hybrid, (b) 30 vol % Pglass hybrid, and (c) 50 vol % Pglass hybrid, all prepared at different melt-mixing speeds.

at 75 rpm displays the lowest modulus as in Figure 4(c). These results can be explained by examining the corresponding micrographs of these materials. The 50% Pglass/polymer hybrid prepared at 50 rpm [Fig. 2(g)] displays some large coalesced structures, but most of the Pglass is dispersed as discrete droplets; the result is that this material has the highest storage modulus. The 50% Pglass/polymer hybrid prepared at 100 rpm hybrid [Fig. 2(h)] shows individual, large Pglass structures, while the 50% Pglass/polymer hybrid prepared at 75 rpm hybrid [Fig. 2(i)] shows a relatively finer, but more interconnected, Pglass phase morphology. This interconnected Pglass phase structure would act as a single large dispersed domain, and thereby causing the lowest storage modulus. A full rheological analysis

TABLE I
Particle Size Distribution for Select Pglass/Polyamide 12 Hybrids Prepared at Different Melt-Mixing Speeds

Melt-mixing speed (rpm)	Mean particle size of 10 vol % Pglass hybrid (μm)	Mean particle size of 30 vol % Pglass hybrid (μm)
50	3.37 ± 0.64	1.71 ± 0.36
75	2.10 ± 0.54	1.18 ± 0.31
100	2.00 ± 0.92	1.24 ± 0.38

of these Pglass/polyamide 12 hybrids is beyond the scope of this paper and will be explored in a future manuscript to be published elsewhere. However, the current work reported in this article has shown conclusive experimental evidence that melt-mixing speed as used here affects both the final morphology and the rheological properties of these unique materials.

Crystalline properties

As a polymeric material is melt-processed to produce a part, it undergoes a transition from the melt (or liquid) to a solid state. Polyamide 12 is a semicrystalline material and will form crystals during this transition from liquid to solid state. As the amount of crystallinity and the speed at which the crystals form impact the final properties of a polymeric material, it is important to understand the effect of Polydrive® melt-mixing speed on these parameters. Percentage crystallinity is usually determined by dividing the observed heat of fusion by the standard heat of fusion for the material. The percentage crystallinity of the hybrid materials was estimated using a slightly modified equation, i.e.,

$$X_c = \frac{(\omega^* \Delta H_{\text{obs}})}{\Delta H_f^o}, \quad (1)$$

where ΔH_{obs} is the heat of fusion observed in the DSC experiment, ΔH_f^o is the standard heat of fusion of a 100% crystalline polyamide 12, and ω is the weight percentage (wt %) of polyamide 12 in the hybrid. The ω term of this equation was added to account for the fact that polyamide 12 is the only crystallizable component of the hybrid. Table II summarizes the percentage crystallinity that was determined for these hybrids. A value of 95 J/g was used as the standard heat of fusion for pure polyamide 12.[27] The observed heat of fusion was obtained from a DSC temperature scan at a heating rate of 10°C/min. It can be seen in Table II that as the content of Pglass is increased, the crystallinity of the system decreases. This experimental observation is consistent with reported studies on Pglass/LDPE and Pglass/Polyamide 6 hybrid systems, where it was shown that the Pglass inhibited crystallite formation.[19,28,29] It is believed that the Pglass is acting similarly in the hybrid system of the present study and is a common feature of hybrid systems. The effect of melt-mixing speed on the percentage crystallinity is negligibly small. There appears to be a slight increase (approximately 1%) in the overall crystallinity when comparing the hybrids prepared at Polydrive® mixing speed of 50 rpm with that prepared at 75 rpm and 100 rpm. The slight increase in the overall crystallinity just mentioned could be within the accuracy of the DSC instrument.

TABLE II
Percentage Crystallinity of Pglass/Polyamide 12 Hybrids Prepared at Different Melt-Mixing Speeds

Vol % polymer	50 rpm X_c	75 rpm X_c	100 rpm X_c
100%	54% ± 1.98%	54% ± 1.98%	54% ± 1.98%
90%	28% ± 0.32%	27% ± 1.11%	29% ± 0.33%
80%	16% ± 1.74%	16% ± 0.80%	15% ± 0.57%
70%	8% ± 0.19%	9% ± 0.17%	9% ± 0.17%
60%	4% ± 0.12%	5% ± 0.05%	5% ± 0.07%
50%	3% ± 0.22%	3% ± 0.06%	3% ± 0.26%

Although the percentage crystallinity of the hybrid was unaffected by the Polydrive® melt-mixing speed, the rate at which the crystals grow and how they grow was impacted. The two parameter Avrami equation was used to describe the crystallization kinetics of these systems as it has been used successfully by many different researchers on many different systems, including polyamide 12.[30–32] The Avrami equation [eq. (2)] describes the percentage crystallinity of a system as a function of time, t, and temperature, T:

$$X_c(t, T) = 1 - \exp[-(kt)^n], \quad (2)$$

where X_c is the degree of crystallinity and k and n are constants. The constant k is the propagation rate constant of the crystal, and it has units of reciprocal seconds, while n is a dimensionless number that depends on the nucleation, geometry, and control of the growth process of the crystal. For the isothermal tests, the sample was heated to 220°C, where it was held for 3.5 min to eliminate previous thermal history. The sample was then quenched to 160°C, where it was held for 17 min. For the Pglass/polyamide 12 hybrid system, only measurements performed at 160°C displayed isotherms that were suitable for Avrami analysis. Other temperatures were examined, but the crystallization peak was either unobservable or very broad. The results of these tests are summarized in Table III.

The calculated value of n for the pure polyamide 12 is consistent with reported values for pure polyamide 12.[33] The growth factor is relatively unaffected by the melt-mixing speed for hybrids with $\leq$ 20% Pglass concentration. These hybrids, except for the 10% Pglass/polymer prepared at 50 rpm, displayed n values of > 3.43. Values of $n > 3.43$ are indicative of athermal nucleation, with three-dimensional growth in a sheaf-like geometry.[34] The 10% Pglass/polymer hybrid prepared at 50 rpm displayed an n value of 2.86, indicating that the shape of the crystal changed from a sheaf to a sphere. It is likely that the consistently poor isotherm at the test temperature observed for the composition just mentioned is the cause of the deviation of the n value. The remaining hybrids that were prepared at 50 rpm were all observed to display an n value greater than

TABLE III
Avrami Parameters for Pglass/Polyamide 12 Hybrids Prepared at Different Melt-Mixing Speeds

Vol % glass	50 rpm		75 rpm		100 rpm	
	Slope (n)	k (s^{-1})	Slope (n)	k (s^{-1})	Slope (n)	k (s^{-1})
0	5.03	1.67×10^{-11}	5.03	1.67×10^{-11}	5.03	1.67×10^{-11}
10	2.86	6.28×10^{-8}	3.85	3.41×10^{-9}	3.43	2.19×10^{-8}
20	3.55	2.63×10^{-8}	3.50	1.07×10^{-7}	3.50	2.09×10^{-7}
30	3.94	1.99×10^{-9}	3.70	7.02×10^{-9}	3.10	1.48×10^{-6}
40	3.93	5.22×10^{-9}	3.99	7.47×10^{-9}	2.64	1.03×10^{-5}
50	4.58	3.50×10^{-10}	3.24	5.03×10^{-9}	2.35	1.2×10^{-5}

3.5 that corresponds to no change in the growth process. As the melt-mixing speed is increased to 75 rpm, the growth of the crystals in the 50 vol % Pglass/polymer hybrid is impacted. This last hybrid composition has an n value approaching 3, which again indicates a shift to a more spherical growth like geometry. As the melt-mixing speed was further increased to 100 rpm, the n value changes at relatively low Pglass concentrations. At 30 vol % Pglass concentration in the hybrid, the n value is changed to 3.10, and it reduces further as the Pglass concentration is increased. For the 50 vol % Pglass/polymer hybrid, the n value indicates another change in the growth process to two-dimensional growth in a circular geometry. The opacity of the Pglass hybrids prevented visual confirmation of the growth factors through polarized light microscopy.

The growth rate of the crystals was also affected by composition and melt-mixing speed. In general, the Pglass acts as a nucleating agent for the growth of the polymer crystals. In contrast to typical nucleating agents, Pglass merely accelerates the growth of the crystals; it does not induce the formation of new crystals. The nucleating effect of the Pglass was reported by Guschl and colleagues[19,28] for low-density polyethylene and polypropylene hybrid systems. However, the nucleation effect of the Pglass is affected by its concentration in the Pglass/polyamide 12 hybrid systems. The melt-mixing speed also impacts the growth rate. In both hybrids prepared at 50 rpm and 75 rpm, the Pglass causes a nucleation effect that reaches its maximum at a Pglass concentration of 20 vol %. As the Pglass concentration is increased further, the growth rate slows down slightly. When the melt-mixing speed is increased to 100 rpm, the growth rate does not reach a maximum at 20 vol % Pglass, but continues to increase with increasing Pglass content in the hybrids. In summary, the crystalline properties of the Pglass/polyamide 12 hybrids described above suggest that melt-mixing speed as used in this study does not significantly affect the overall crystallinity of the hybrid material. However, the shape and growth rate of the crystals is greatly impacted by the melt-mixing speed of the material, thereby leading to the conclusion that the amorphous Pglass phase in the hybrids greatly influences the growth of the polyamide 12 crystals in the hybrid systems studied. These crystallinity results also suggest that any observed influence of the melt-mixing speed on the hybrid mechanical properties (discussed below) can be ascribed solely to the overall morphology of the hybrid material.

Tensile properties

Mechanical properties play a large role in determining if a material can be used for a certain application. The mechanical properties of a polymer blend depend on the individual component properties, blend composition, and on the final morphology of the material. Polymer composite properties depend on factors such as the type of filler, concentration of filler, and how the filler is arranged in the material, i.e., packing fraction. The Pglass/polymer hybrids of the present study fit in between these two types of polymeric materials. As already discussed, the mode of Pglass dispersion inside the polymer matrix of the hybrids encompasses a number of different morphologies similar to that reported for typical polymer blends. However, the Pglass phase after solidification of the hybrid is a rigid inorganic glass at room temperature in remarkable contrast to classical polymer blends. By systematically investigating the effect of melt-mixing speed on the hybrid tensile properties, the processing/structure/property relationship of this important class of polymeric materials can be understood. This understanding is crucial to controlling the fabrication of Pglass/polymer hybrid parts with reproducible properties for a number of applications.

Figure 5 shows typical stress/strain curves for the Pglass/polyamide 12 hybrid materials studied. The pure polyamide 12 displays typical polymer behavior with a clearly defined yield stress. As Pglass is added to the system, the yield stress disappears and the curves begin to resemble that of brittle solids. Table IV shows the effect of melt-mixing speed on

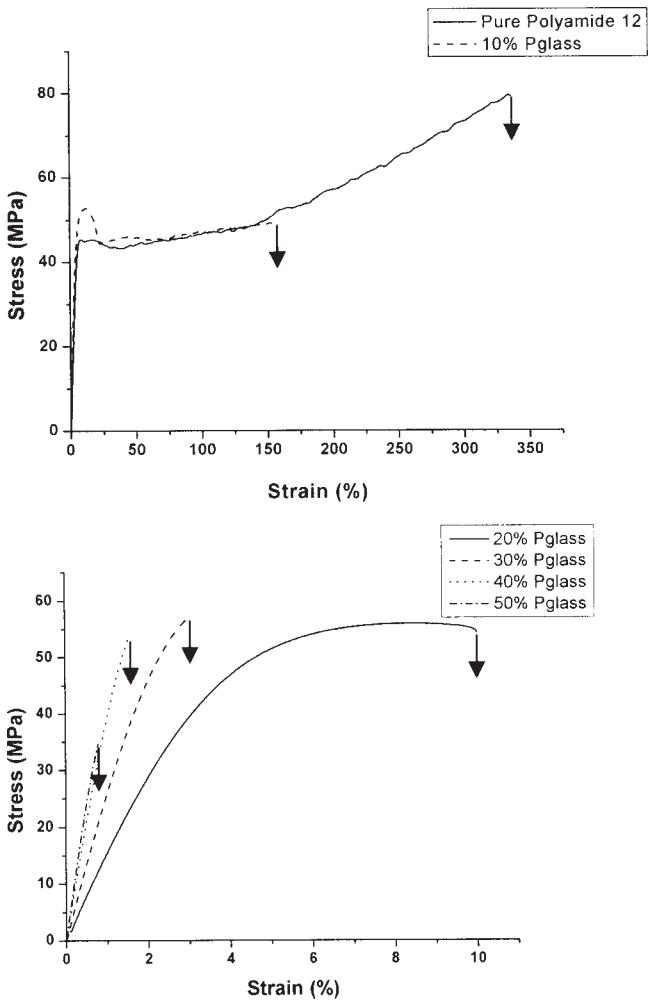

Figure 5 Typical stress/strain curves for Pglass/polyamide 12 hybrids.

strain at break. The hybrids melt-mixed in the Polydrive® at 50 rpm display the highest strain at break for all the hybrid compositions while the hybrids melt-mixed at 100 rpm display the lowest strain at break for compositions containing less than 20 vol % Pglass. The observed trend changes at the higher Pglass concentrations, where the hybrids melt-mixed at 100 rpm have ultimate strains approaching that of the hybrids melt-mixed at 50 rpm. While the hybrids melt-mixed at 75 rpm tended to exhibit the lowest strain at break, they also tended to have the highest modulus of the materials as can be seen in Figure 6.

While it is clear from the preceding discussion that the hybrid materials melt-mixed at 75 rpm are best for high stiffness applications and the hybrids melt-mixed at 50 rpm and 100 rpm show a slightly lower stiffness and more strain at break, it is more important to be able to predict the behavior of these materials from the properties of the hybrid components. The Halpin–Tsai equation [eq. (3)] is a useful relationship used by many researchers to accurately predict the modulus of a polymer reinforced by a rigid filler:[35]

$$E_c = E_m\left(\frac{1 + AB\phi_f}{1 - B\psi\phi_f}\right), \tag{3}$$

where E_c is the predicted modulus of the composite, E_m is the modulus of the polymer matrix, and φ_f is the volume fraction of filler in the system. The constant A accounts for the Poisson's ratio of the matrix and the geometry of the filler. In the case of spherical fillers A is expressed as shown in eq. (4), where ν_m is the Poisson's ratio of the matrix:

$$A = \frac{7 - 5\nu_m}{8 - 10\nu_m}. \tag{4}$$

The constant B depends on the relative moduli of the filler (E_f) and matrix phases and is defined in eq. (5):

$$B = \frac{\frac{E_f}{E_m} - 1}{\frac{E_f}{E_m} + A}. \tag{5}$$

The factor ψ can be approximated by eq. (6), assuming the modulus of the filler is significantly greater than that of the polymer and if the Einstein coefficient is much greater than 1.0:

$$\psi = 1 = \frac{\phi_m}{p}[p\phi_f + (1 - p)\phi_m]. \tag{6}$$

In eq. (6), p is the maximum packing fraction of the filler. The Poisson's ratio is one of the unknown variables in the preceding equations. A polymer above its T_g is often assumed to have a Poisson ratio of 0.5.[36] However, the polyamide 12 is below its T_g at room temperature. An effective Poisson's ratio can be calculated for a filled system as shown in eq. (7):[37]

$$\nu_e = \nu_m - \frac{2(\nu_m - \nu_f)(1 - \nu_m^2)}{[\phi_f(1 - \nu_m - 2\nu_m^2) + (1 + \nu_m)]}\phi_f, \tag{7}$$

TABLE IV
Strain at Break for Pglass/Polyamide 12 Hybrids Prepared at Different Melt-Mixing Speeds

Vol % Pglass	Strain at break (%)		
	50 rpm	75 rpm	100 rpm
0	318.34 ± 46.10	318.34 ± 46.10	318.34 ± 46.10
10	159.11 ± 65.37	113.93 ± 64.06	13.21 ± 8.15
20	8.23 ± 0.97	5.00 ± 0.49	4.34 ± 0.49
30	2.68 ± 0.51	1.63 ± 0.26	2.69 ± 0.36
40	1.56 ± 0.13	0.84 ± 0.10	1.30 ± 0.22
50	0.76 ± 0.23	0.60 ± 0.04	0.94 ± 0.14

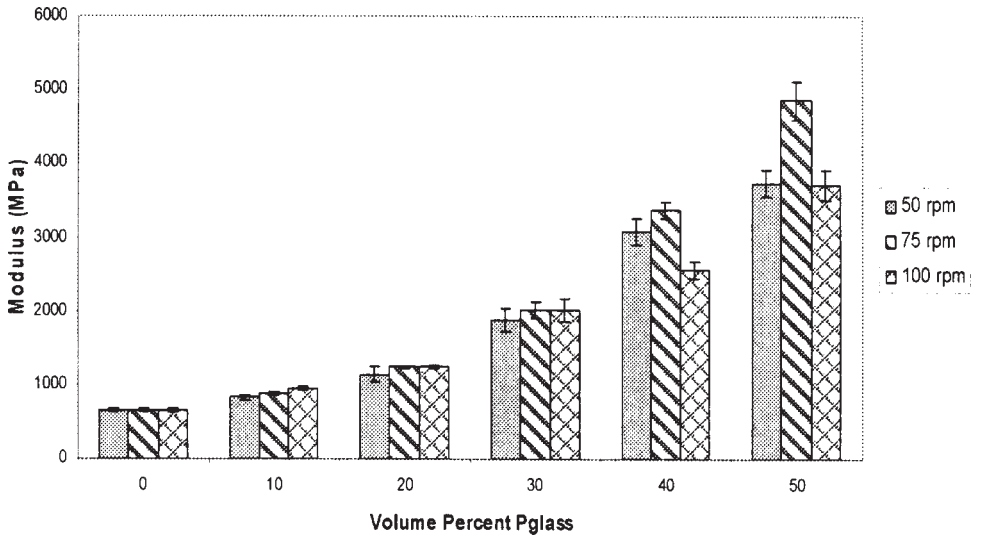

Figure 6 Young's modulus for Pglass/polyamide 12 hybrids melt-mixed at different speeds.

where ν_f is the Poisson's ratio of the filler. All the quantities in eq. (3), except for the packing fraction, are known or can be calculated using the above equations and measured values of 0.655 GPa and 29.29 GPa for the matrix (polyamide 12) and filler (Pglass) moduli, respectively. The Poisson's ratio for the pure polyamide 12 and the Pglass are 0.35 and 0.25, respectively.[38] By systematically varying the unknown packing fraction, the theoretical (calculated) modulus of the hybrid can be brought within 2% of the measured hybrid modulus. The packing fractions used to achieve such a result are shown in Table V. The 10 vol % Pglass hybrids all display packing fractions that have physical meanings corresponding to face-centered cubic packing (50 rpm hybrid), simple cubic packing (75 rpm hybrid), and random close packing, agglomerated (100 rpm) respectively.[35] The 20 vol % melt-mixed at 50 rpm hybrid displays a packing fraction that corresponds to a filler distribution that is random close packing, nonagglomerated. The packing fraction values of the other hybrids fall between 0.355 and 0.49. By using weighted averages of the calculated packing fractions, it should be possible to accurately calculate a modulus for any polyamide 12 hybrid that contains 10–50 vol % Pglass prepared at any speed between 50 and 100 rpm. The weighted packing fraction averages just mentioned are thought to be reasonable estimates of the unknown packing fractions of the actual complex heterogeneous structures (agglomerated/nonagglomerated randomly packed) of the hybrids already discussed.

The novel hybrid materials of this study are known to exhibit complex interpenetrating and co-continuous microstructures unrealizable in conventional mineral filler reinforced polymers as already discussed. At ambient conditions, the hybrids are comprised of very rigid inorganic Pglass phase and a relatively weak, viscoelastic organic polymer phase. As a result, the difference between the stiffness of the individual constituent phases can be several orders of magnitude. Furthermore, because of the partial miscibility of the constituent phases, the local properties can vary in a nontrivial manner across the interfaces.[3,22,29] It is precisely a combination of all these factors that brings about the interesting and advantageous properties of the present hybrids. But it is also the same factors that make it so difficult to develop accurate theoretical equations for predicting the properties of the hybrids.

It is noteworthy that accurate rational models have been developed for predicting elastic properties of two-phase composites with spherical, ellipsoidal and infinitely long cylindrical inclusions.[39] However, in most cases this rational theoretical analysis has been limited to the domain of dilute filler concentrations, where one can effectively neglect the interactions between the inclusions. Recently, a generic finite-element based approach for predicting the behavior and properties of multi-phase materials composed of anisotropic, arbitrarily shaped and oriented phases has been reported by Gusev and colleagues.[40,41] In a future proposed research, the finite element procedure of Gusev will be extended to allow for the rational com-

TABLE V
Packing Fractions of Different Pglass/Polyamide 12 Hybrids Prepared at Different Melt-Mixing Speeds

Vol % Pglass	Packing fraction		
	50 rpm	75 rpm	100 rpm
10%	0.7405	0.5236	0.37
20%	0.632	0.49	0.49
30%	0.42	0.385	0.39
40%	0.38	0.355	0.46
50%	0.465	0.375	0.47

puter-aided design of novel Pglass/polymer hybrid systems.

CONCLUSIONS

Phosphate glass/polymer hybrids belong to an extraordinary and relatively new class of materials that combines the benefits of conventional polymer blends and glass-filled composites. While the full utility of these materials has yet to be realized, important steps in fully understanding these materials are being taken. This study is the first attempt to elucidate a processing/structure/ property relationship for the Pglass/ polyamide 12 hybrid materials. By studying the effect of melt-mixing speed on the liquid state, via rheology; the transition between liquid and solid states, via crystallization properties; and solid state physical properties, this study will be useful to understand the complex interplay of the hybrid morphology and properties during processing. This study revealed an increase in hybrid viscosity with increasing Pglass concentration. As expected, the effect of processing conditions, which dramatically affects morphology, also impacted the rheology of individual compositions. It was also determined that melt-mixing speed did not affect the overall crystallinity of the hybrid systems, but it played a large role in determining the crystallization parameters of the material. Further, we were able to elucidate the effect of melt-mixing speed on the hybrid tensile properties. The Halpin–Tsai equation was successfully applied to these materials, providing a foundation for predicting the final properties of hybrids based on the hybrid component properties and processing conditions. Although Pglass/polymer hybrids have not realized their full technological potential, further studies that detail their unique properties will allow these scientifically interesting and industrially useful materials to bridge the gap between currently available materials and new material needs.

K.U. thanks the Hearin Foundation for graduate student fellowship support and the Moore Research Group for the use of their Materials Testing System. The research work of J.U.O.'s former graduate and postdoctoral students is gratefully acknowledged.

References

1. Nandan, B.; Kandpal, L. D.; Mathur, G. N. J Polym Sci Part B: Polym Phys 2004, 42, 1548.
2. Loy, D. A. MRS Bull 2001, 26, 364.
3. Tischendorf, B. C.; Harris, D. J.; Otaigbe, J. U.; Alam, T. M. Chem Mater 2002, 14, 341.
4. Otaigbe, J. U.; Beall, G. H. Trends Polym Sci 1997, 5, 369.
5. Brow, R. K. Structure, Properties and Applications of Phosphate and Phosphate-Containing Glasses; University of Missouri: Rolla, MO, 1999.
6. Tick, P. A. Phys Chem Glasses 1984, 25, 149.
7. Xu, X. J.; Day, D. E. Phys Chem Glasses 1990, 31, 183.
8. Xu, X. J.; Day, D. E. Brow, Callahan, R. K. P. M. Phys Chem Glasses 1995, 36, 264.
9. Jeon, H. K.; Kim, J. K. Polymer 1998, 39, 6227.
10. Veenstra, H.; van Lent, B. J. J.; van Dam, J.; de Boer, A. P. Polymer 1999, 40, 6661.
11. Lee, J. K.; Han, C. D. Polymer 1999, 40, 6277.
12. Trongsatitkul, T.; Aht-Ong, D.; Chinsirikul, W. Macromol Symp 2004, 216, 265.
13. Tucker, C. L., III; Moldenaers, P. Annu Rev Fluid Mech 2002, 34, 177.
14. Roland, C. M.; Bohm, G. G. A. J Polym Sci Part B: Polym Phys 1984, 22, 79.
15. Burkhart, B. E.; Gopalkrishnan, P. V.; Hudson, S. D.; Jamieson, A. M. Phys Rev Lett 2001, 87, 098301.
16. Vazquez, M. O.; Gloria Bello, O.; Gonzalez-Nunez, R.; Arellano, M.; Moscoso, F. J. SPE Antec Tech. Pap 2004, 62, 2097.
17. Frayer, P. D.; Monahan, R. J.; Pierson. M. D. Corning U.S. Pat. 6,103,810 (2000).
18. Young, R. T.; McLeod, M. A.; Baird, D. G. Polym Compos 2000, 21, 900.
19. Guschl, P. C.; Otaigbe, J. U.; Taylor, E. P. SPE Antec Tech Pap 2003, 61, 2137.
20. Otaigbe, J. U.; Quinn, C. J.; Beall, G. H. Polym Compos 1998, 19, 18.
21. Guschl, P. C.; Otaigbe, J. U. J Colloid Interface Sci 2003, 266, 82.
22. Rawal, A.; Urman, K.; Otaigbe, J.; Schmidt-Rohr, K. Chem Mater 2006, 18, 6333.
23. Adalja, S. B.; Otaigbe, J. U;. Thalacker, J. Polym Eng Sci 2001, 41, 1055.
24. Urman, K.; Otaigbe, J. U. SPE Antec Tech Pap 2004, 62, 2063.
25. Vinckier, I.; Moldenaers, P.; Mewis, J. J Rheol 1996, 40, 613.
26. Taylor, G. I. Proc R Soc London Ser A 1932, 138, 41.
27. Gogolewski, S.; Czerniawska, K.; Gasiorek, M. J Colloid Polym Sci 1980, 258, 1130.
28. Guschl, P. C.; Otaigbe, J. U. J Appl Polym Sci 2003, 90, 3445.
29. Urman, K.; Otaigbe, J. U. J Polym Sci Part B: Polym Phys 2006, 44, 441.
30. Park, C.-S.; Lee, K.-J. Nam, J.-D.; Kim, S.-W. J Appl Polym Sci 2000, 78, 576.
31. Liu, M.; Zhao, Q.; Wang, Y.; Zhang, C.; Mo, Z.; Cao, S. Polymer 2003, 44, 2537.
32. Plummer, C. J. G.; Zanetto, J.-E.; Bourban, P.-E.; Manson, J.-A. E. Colloid Polym Sci 2001, 279, 312.
33. Chuah, K. P.; Gan, S. N.; Chee, K. K. Polymer 1998, 40, 253.
34. Gedde. U. W. Polymer Physics; Kluwer: Boston, 1999; p 169.
35. Nielsen, L. E.; Landel, R. F. Mechanical Properties of Polymers and Composites; Marcel Dekker: New York, 1994.
36. Flandin, L.; Chang, A.; Nazarenko, S.; Hiltner, A.; Baer, E. J Appl Polym Sci 2000, 76, 894.
37. Uschitsky, M.; Suhir, E.; Kammlott, G. W. J Electron Packaging 2001, 123, 260267.
38. Brandrup, J.; Immergut, E. H., Eds. Polymer Handbook; John Wiley & Sons: New York, 1989.
39. Christensen, R. M. Mechanics of Composite Materials; Krieger: Malabar, FL, 1991.
40. Gusev, A. A. Macromolecules 2001, 34, 3081.
41. Gusev, A. A.; Hine, P. J.; Ward, I. M. J Mech Phys Solids 1997, 45, 1449.